Multimedia Tools and Applications (2020) 79:10405–10425
https://doi.org/10.1007/s11042-019-07891-9

The design of a dual channel synchronous control system based on a new percutaneous puncture surgical robot

Liandong Wang[1] · Tiehua Hu[2]

Received: 19 March 2019 / Revised: 21 April 2019 / Accepted: 10 June 2019 /
Published online: 18 July 2019

Abstract
One type of automatic medical tele-robotics system that is used in Percutaneous Puncture Surgery has been presented in this paper. A compensation (or synchronous) method for physiological movement is a necessary control method to reduce the difficulty of operations and improve operating accuracy for an automatic Percutaneous Puncture Surgical Robot (PPSR). Firstly, the robotics system can put a surgeon away from X-ray radiation. Secondly and importantly, the control system of the Robot is based on an Iterative Learning Control (ILC) algorithm which is a dual channel synchronous control system. The puncture actuator controlling channel is in charge of automatically inserting a needle and compensating for the motion of the internal organs. The robotic arm controlling channel is in charge of controlling the direction of the needle and compensating for the body's external inserting point motion with the on-line supervision. The performance of the control system has been evaluated and simulated in MATLAB. The results have been proven that the control process is effective.

Keywords Dual channel · Synchronous control · Surgical robot · Tele-robotics

1 Introduction

The percutaneous puncture technique is the basis of interventional radiology. Its purpose is to establish a pathway for the completion of both diagnosis and treatment. Currently, the more advanced technology is the image-guided percutaneous puncture technique. The technical scheme of the operation is as follows: Firstly, CT or MRI scanners are used to acquire the image data of the patient's focus area, and then the three-dimensional information of the

✉ Liandong Wang
wangliandong_jlu@163.com

[1] School of Mechanical and Aerospace Engineering (SAME), Jilin University, Changchun, China

[2] China Academy of Machinery Science & Technology (CAM), Beijing, China

patient is obtained by image reconstruction. Secondly, according to the image information, the doctor carries on the path planning before the operation, the doctor then selects the puncture inserting point and marks it on the skin of the patient. Thirdly, the doctor holds the puncture needle, and then adjusts the direction of the puncture needle to meet the requirements of the needle's inserting path with the help of the visual sensor of the navigation system after the puncture surgical system calculating the spatial position. Finally, the doctor inserts the needle and completes the operation.

There are some shortcomings in the current surgical technology scheme, which are as follows: (1) Any tremor in the doctor's hand directly affects the quality of the operation because the doctor holds the puncture needle all the time. (2) Doctors have to suffer a lot of X-ray irradiation damage during the time when the CT equipment is operating. (3) Due to some difficult operations, patients will inevitably carry out appropriate physiological movements [3] during the long operating time. In the patient's body [8], internal organic physiological movements will be more complex, and the focus area may produce great change location and volume due to physiological movement. During doctor operating, the doctor cannot ensure that the relative position of the puncture end of the needle and the area of focus will remain unchanged, that is to say, the doctor cannot keep the same frequency and the same range of movement as the patient's physiological movement. Consequently, the quality of operation will be reduced or even failed.

Recently there have been a number of papers that have been presented in the literature, in which many solutions to the problems mentioned above have been proposed. Mojtaba Sharifi [15] proposed that a Master Impedance Model and a Slave Impedance Model be added into the tele-robotic control system. Appropriate filters and filter devices are used to improve the accuracy of surgical robots as has been described in some the literature. Ginhoux R. et al. [5] proposed an optimized filter used to incorporate the generalized predictive controller (GPC) system to deal with the influence of physiological movement on the surgical robots. Rogerio Richa et al. [14] constructed a model of the periodic beating motion of the heart through a novel time-varying dual Fourier series that contained an Extended Kalman Filter. Gabriele Ligorio et al. [9] designed a linear Kalman filter to help an inertial based inclinometer to target to the motion of the heart. Zarrouk Z et al. [19] proposed a force feedback control system to compensating physiological motions in beating heart surgery.

In the literature [16], a control system has been proposed where the system first estimates the motion of the organ with a Kalman filter, and then compensates for the motion to deal with the problems of the delayed, and different measurement rates and the unregistered sensor data. The great range of the organ movement in the body was not able to be solved by the method of designing a filters and devices. There are several methods that are used to help the robotic system deal with physiological motion, such as image compensating methods. Alexandre B. proposed a 3-D reconstruction algorithm for the coronary tree that could deal with motion estimation and motion compensation [1]. Adiyo Prakosa [12] proposed a way that a database could be used to estimate the cardiac electrophysiological activation pattern. Toni Neicu et al. [6] proposed a method which could be used to control the synchronization between the motion of a tumour and the treatment under an X-ray beam to derive the average tumour trajectory (ATT) from the measured tumour trajectory data. Michel Dominici et al. [4] proposed a two loop cascade merging algorithm. The algorithm contains an inner loop that performs adaptive model control and an outer loop that compensates for the beating motion of the heart based on model predictive control (MPC). These methods were not suit of CT equipment. Because image reconstruction was very slow, the robotic arm could not synchronize with image reconstruction. Martin J. Murphy [10] proposed a Tracking Moving Organs method that can be used in the Cyberknife system in real time. However, this method needs a lot of data to compute the outputs and the device is very expensive. Researchers proposed control system

compensation methods. Nakamura Y. et al. [11] developed a motion canceling robot system that contained a visual synchronizing system that received visual information from a camera, a motion synchronizing system and a master-slave control system. Franck P. Vidal et al. [17] presented a framework that combined evolutionary optimization, soft tissue modelling and ray tracing on GPU to simultaneously compute the respiratory motion and X-ray imaging in real-time. Bruno D. et al. [2] proposed a machine learning algorithm used in the positional learning controller for MIS. The pathway can be estimated through the use of previous data with the machine learning algorithm. Inoue T. et al. [7] proposed a 3-DOF dual delta-type parallel IVR robot and this robot is able to operate together with CT. Other researchers have designed the structure platform. Nathan A. Wood et al. [18] proposed a stable operating platform where the robot platform adheres to, and crawls over, the surface of the heart. Therefore the platform could maintain synchronization with the motion of the heart. However, control systems and platform mentioned above could not deal with difference range of external and internal organ movement.

The article has been organized as follows: the automatic medical tele-robotics model has been used in this article has been described. A dual channel synchronous control system based on an Iterative Learning Control (ILC) algorithm has been presented and two channel respective functions have been illustrated. The performance of the control system for an automatic Percutaneous Puncture Surgical Robot (PPSR) has been illustrated, followed by the conclusion.

2 Automatic needle insertion puncture robot model

This paper has presented a medical tele-robot system, as shown in Fig. 1, which can automatically insert a needle and synchronize with physiological movement with online supervision. This system has first put forward a fully automatic needle insertion system. Secondly, a method for synchronizing the puncture movement and the patient's physiological motion has been put forward, as shown in Fig. 2, Fig. 3 and Fig. 4.

Physiological movements mainly involve breathing movements and the beating of the heart. The amplitude of the external point of a normal person's breathing movement has been shown in Fig. 5. It can be seen from Fig.5 that the period of respiratory movement is stable.

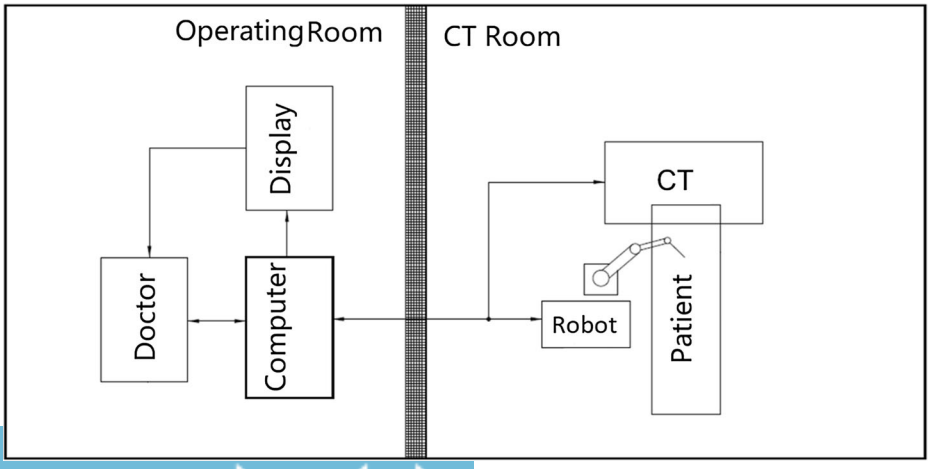

Fig. 1 The automatic needle insertion puncture robotic system

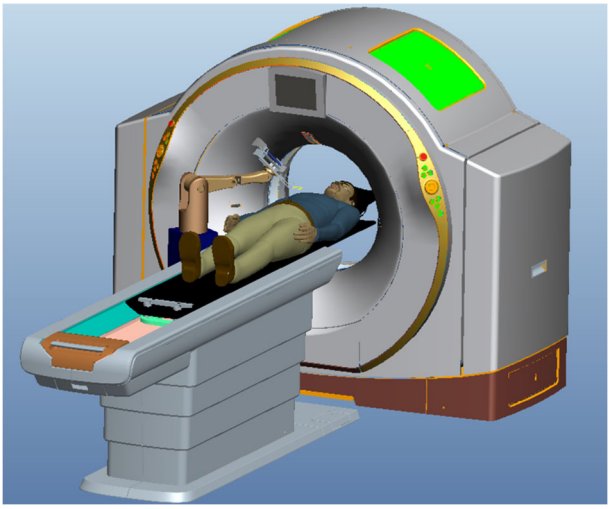

Fig. 2 The automatic needle insertion puncture robotic model

The data diagram of the respiratory motion shown in Fig.5 can be obtained by setting the appropriate sampling frequency. The beating of the heart is more complicated than the breathing movement. From the literature [5], the cycle of the heart beat of a pig is about 0.625 s, with a frequency of 1.6 Hz. From general statistics of people, the heart beat frequency is 70 *b*/*m*, and the cycle is 0.85 s. The heart beat is also periodic and stable. In order to ensure the quality of the operation and relieve the pain of the patient, it is necessary to anaesthetize the patient and to keep the patient breathing steadily through the use of breathing apparatus. Therefore the patient's breathing and heart beat would be smoother.

3 Control system

In this paper, a 7-DOF robot has been proposed, as shown in Fig. 2. The robot is composed of two parts, one is the 6-DOF robot arm for approaching the needle insertion point and controlling the needle direction, the other is the 1-DOF automatic needle insertion actuator. In the two parts mentioned above, the first part is used to control the direction of the entry point

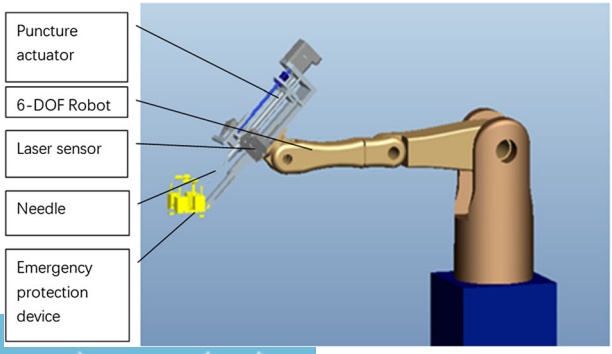

Fig. 3 The automatic needle insertion puncture robot arm and actuator

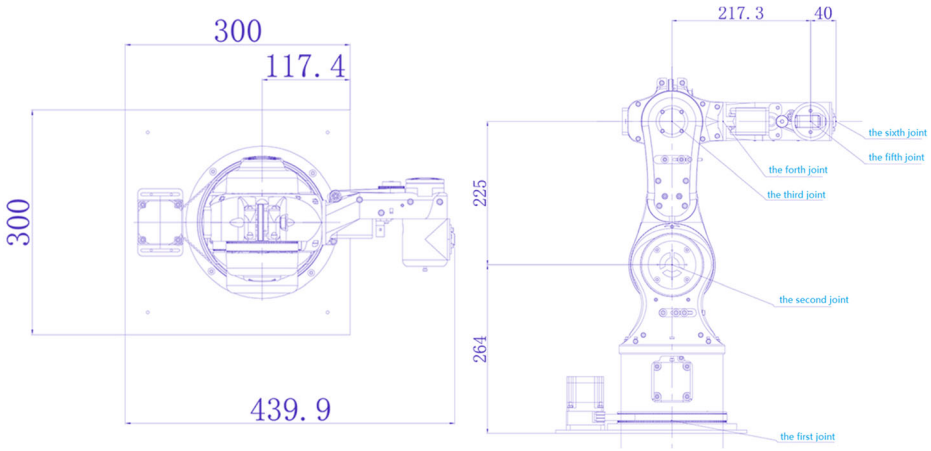

Fig. 4 The dimensions of the robotic arm (mm)

and compensate for the motion of the patient. The second part controls and compensates for the physiological movement of the intra-corporeal organs.

According to the literature, there are many control systems that have been used as a surgical robot control system. There are control systems based on force feedback or position feedback, a traditional PID control system, a model predictive control system, a repetitive predictive control system and a neural network control system and so on. Moreover the feedback modes of these systems are also different, such as force feedback, position and distance feedback, image feedback and so on. There are many methods for dealing with physiological movements, such as filter methods, fixed structural platform methods and trajectory prediction methods and so on.

The following considerations should be taken into account when designing a robotic control system.

1. It is necessary to analyze the mechanical and structural characteristics of the robotic actuators. The characteristics of the actuator affect the design of the surgical robot control system.
2. Image Acquisition Method should be fully taken into account. For example, the scanning field of CT is small and the image is sliced. If real time imaging is required, there must be a number of X - ray acquisitions, and the CT bed will be moving at all times. If an ultrasonic device is used to acquire images, the detection equipment must be in contact with the human body and there must be no cavity in the abdomen filled with air. If a camera is used to acquire image data, then the image is 2D, and there is no 3D information. The trajectory prediction cannot be carried out according to its image data.
3. The frequency of image acquisition should be taken into consideration, because CT equipment needs the CT bed to move when collecting data, therefore the acquisition frequency is very low. However the MRI bed cannot be moved and the manufacturing cost of the surgical robot is greatly increased because of the strong magnetic field.
4. The control system should take into account the method to position the needle, such as a binocular camera, magnetic signal position feedback or laser distance sensor feedback and so on.

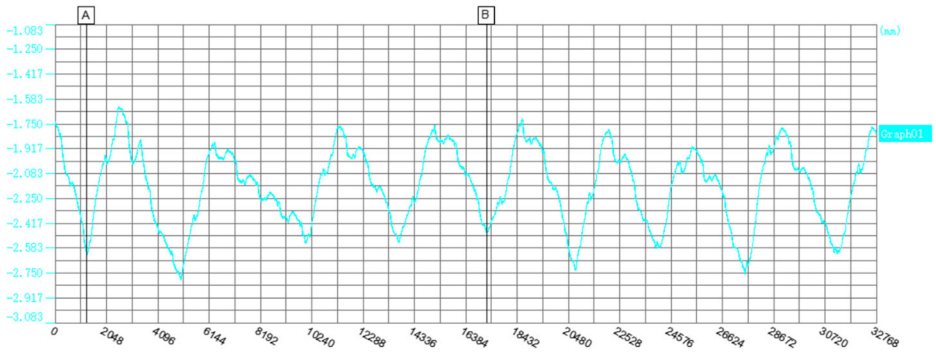

Fig. 5 Motion for one point of the body (data from the Keyence LK-G5000)

5. It is also important to consider whether the position of the robot can be acquired in real time. If it is necessary to acquire it in real time, trajectory planning and tracking can be carried out. The percutaneous puncture robot system has been shown in the following Figure 6:

4 Path planning system

According to the structure of the robot and the characteristics of the control system mentioned above, an dual channel Iterative Learning Control (ILC) algorithm has been proposed that is able to be used to plan the path and compensate for the complex physiological movements of organs, such as respiration and heart beating. The first channel ILC is able to learn the external point (the needle inserting point) moving path, and the second channel ILC is able to learn internal point (organ focus point) moving path.

The introduction of the iterative learning control algorithm (ILC):

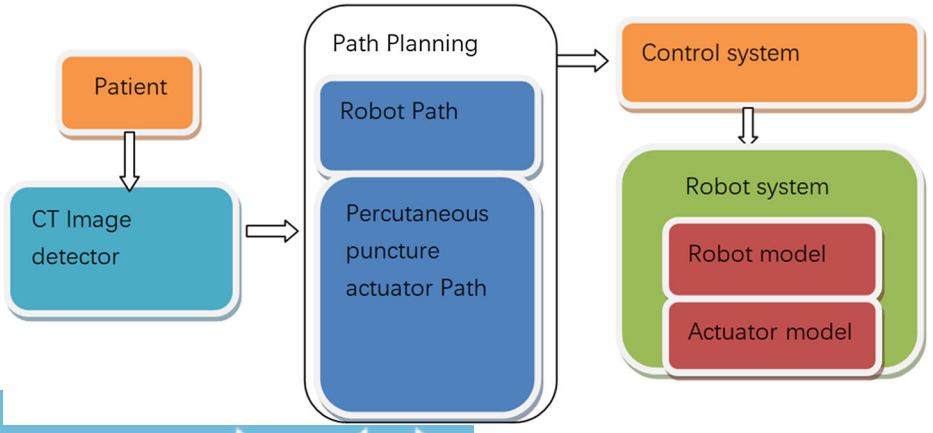

Fig. 6 The percutaneous puncture robot system

The state equation and the output equation of the ILC:

$$\dot{x}(t) = f(x(t), u(t), t)$$
$$y(t) = g(x(t), u(t), t)$$

According to the Iterative learning control algorithm and after running it many times, the system will get the result that: Control Input $u_k(t) \rightarrow u_d(t)$ and system output $y_k(t) \rightarrow y_d(t)$.

The equation of the state for k iterations:

$$\dot{x}_k(t) = f_k(x(t), u_k(t), t)$$

The output of the equation for k iterations:

$$y_k(t) = g(x_k(t), u_k(t), t)$$

The error at this time is:

$$e_k(t) = y_d(t) - y_k(t)$$

$e_k(t)$ is the error of $y_d(t)$ between$y_k(t)$.

The closed-loop learning control algorithm is:

$$u_{k+1}(t) = L(u_k(t), e_{k+1}(t))$$

From the equation, the $k+1$ iteration input is equal to the k iteration input added to the $k+1$ output error in the closed-loop learning control system.

Description of the parameters in the equations:

$x \in R^n$ - A state variable of the system.

$y \in R^m$ - An output variable of the system.

$u \in R^r$- An input variable of the system.

$f(\cdot)$ - State function for the proper dimensions.

$g(\cdot)$ - Output function for the proper dimensions.

$u_d(t)$ - The expected control input.

$y_d(t)$ - The expected output.

$x_k(0)$ - The initial state of each run.

$t \in [0, T]$ - The system time.

L - An operator that may be linear or nonlinear.

$y_k(t)$ - The k iteration output for the system.

5 Robot trajectory planning object

The dynamic performance of an N- joint robot can be described by a second order nonlinear differential equation. The robotic arm contains 6-DOF, and the puncture actuator is described as a 1-DOF robot where the $C(q, \dot{q}) \in R^n$ and $G(q) \in R^n$ of which are zero.

$$M(q)\ddot{q} + C\left(q, \dot{q}\right)\dot{q} + G(q) = \tau - \tau_d$$

$q \in R^n$ - Angular displacement of the joint.

$M(q) \in R^{n \times n}$ - The inertial matrix of the robot.

$C(q, \dot{q}) \in R^n$ - Centrifugal force and Coriolis force.

$G(q) \in R^n$ - Gravitational term.
$\tau \in R^n$ - Control torque.
$\tau_d \in R^n$ - Errors and disturbances.
The learning control function of the closed loop PD type for the system above is:

$$u_{k+1}(t) = u_k(t) + K_p\left(q_d(t) - q_{k+1}(t) + K_d\left(\dot{q}_d(t) - \dot{q}_{k+1}(t)\right)\right.$$

Where:

K_p Proportions matrix
K_d Differential matrix

6 The process for path planning

During the CT image acquisition, two CT scans are performed for the location of the focus, the first scan is at the end of expiration, and the second scan is at the end of inhalation. ${}^{CT}_{f}P1$ and ${}^{CT}_{f}P2$ are the locations for two types of scans mentioned above.

Where:

${}^{CT}_{f}P1$ the first focus location for the coordinates of the CT
${}^{CT}_{f}P2$ the second focus location for the coordinates of the CT

At the same time, it is necessary to mark the spatial position of the robot's front marker, M, in the CT image that has been shown in the Fig. 7. Through 3D imaging of the CT device, and the four balls on the marker M, the spatial coordinates ${}^{CT}_{M}P1$、${}^{CT}_{M}P2$、${}^{CT}_{M}P3$ and ${}^{CT}_{M}P4$can be obtained. Then the O_M coordinate system of the marker can be established through the use of a certain algorithm. In the coordinate system the focus points ${}^{CT}_{f}P1$ and ${}^{CT}_{f}P2$ are transformed to ${}^{M}_{f}P1$ and ${}^{M}_{f}P2$ under the coordinate systemO_M.

Moreover, the marker M on the front of the robot is fixed to the mechanical arm. The geometric size of the marker M is determined with the manipulator. At the same time, an absolute angle position sensor is located at each joint of the robot, and the position and orientation of the robot can be known at any time by measuring the feedback from these sensors.

Therefore, the coordinate system of a robot is set up to be O_R . ${}^{M}_{f}P1$ and ${}^{M}_{f}P2$ are transformed to ${}^{R}_{f}P1$ and ${}^{R}_{f}P2$ under the coordinate system O_R, as shown in Fig. 8.

At the end of expiration, the appropriate insertion point for a needle (P_{EN}) on the patient's body surface is selected with the help of the 3D image. The marker M2 is pasted to the entry point. At the end of expiration, the coordinate ${}^{R}_{M2}P^{M2}1$ of M2 at the moment in time are obtained through the use of the CT image; then at the end of inhalation, the coordinate ${}^{R}_{M2}P^{M2}1$ of M2 at the moment in time are obtained again. According to the same transformation method, the coordinates ${}^{CT}_{M2}P^{M2}1$ and ${}^{CT}_{M2}P^{M2}2$ of the marker M2 attached to the surface of the patient can be transferred to ${}^{R}_{M2}P^{M2}1$ and ${}^{R}_{M2}P^{M2}2$ in the coordinate system O_R .

The coordinate system of the CT has been shown in Fig. 9.

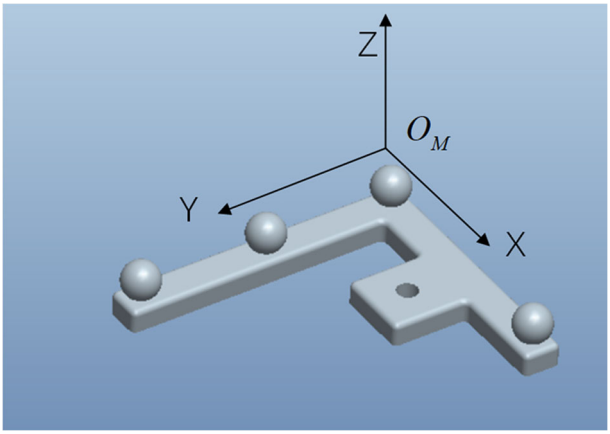

Fig. 7 The coordinate system O_M of the marker M

The system of the puncture robot is decomposed into two parts (Fig. 8), which contain the path planning of the robot and the path planning of the puncture actuator.

One is the 6-DOF robotic arm; the other is the puncture actuator. The robot arm is responsible for tracking the position of the marker point M2 and tracking the target orientation, and the mechanical actuator part is responsible for controlling the distance between the focus point and the point M2.

The PD type learning control algorithm has been adopted to calculate the motion paths of the robot's joints and the actuator at all times in the path planning process. The PD type learning controller is divided into two channels to implement the M2 marking point's learning path planning and the focus learning path planning, respectively.

From Fig. 10 and Fig. 11, it can be seen that the marker M2 acts in a reciprocating periodic cycle motion between the two points ${}^{R}_{M2}P^{M2}1$ and ${}^{R}_{M2}P^{M2}2$ on the surface of the body along with the

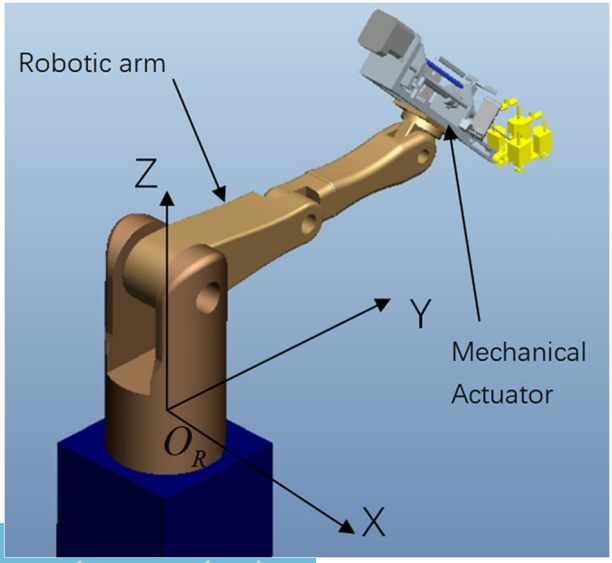

Fig. 8 The coordinate system O_R of the robot

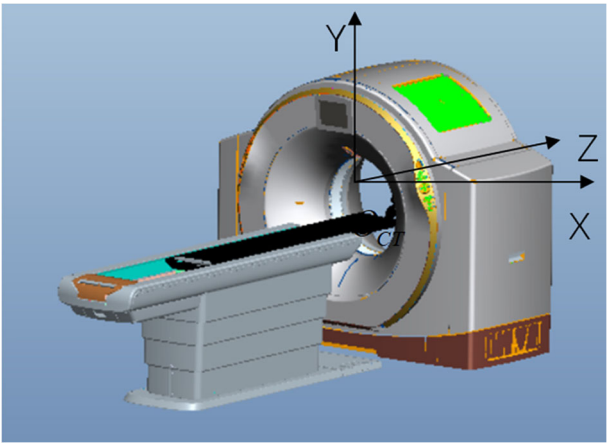

Fig. 9 The coordinate system O_{CT} of the CT

physiological movement. The focus of the lesion periodically moves between the two points ${}^{R}_{f}P1$ and ${}^{R}_{f}P2$ on the surface of the body along with the physiological movement in the body.

7 The control process

There are two planning paths, one is the movement path of the robotic arm, and the other is the movement path of the puncture actuator tip. Finally, the spatial location path of the puncture actuator tip is where the two paths merge together. Thus in order to ensure that the needle tip moves according to the planning process, it is necessary that the location of the needle tip meets the required accuracy at any point in time.

In the path planning stage, it is necessary to consider several problems of the control process of the needle insertion during the later stage of the puncture.

1. The time taken for the action of the mechanical puncture actuator is important. The needle acts at the time of the physiological movement when the puncture operation is carried out.
2. After the puncture starts, it is important to control each puncture of the needle tip of the robotic arm on the puncturing path and its position in space at any time and reach the desired position of the system due to the dual channel path planning and dual channel control system.

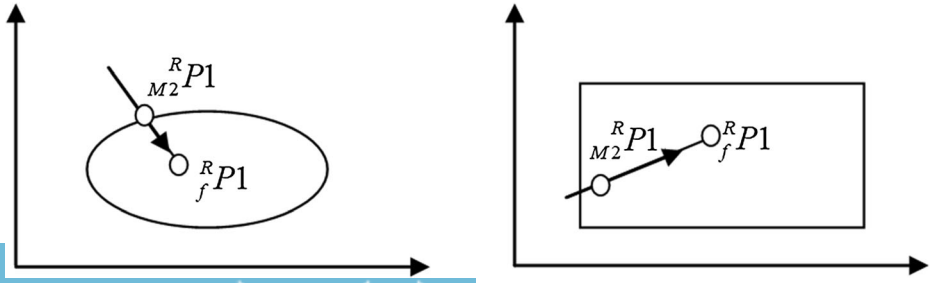

Fig. 10 ${}^{R}_{M2}P^{M2}1$ and ${}^{R}_{f}P1$ at the end of expiration

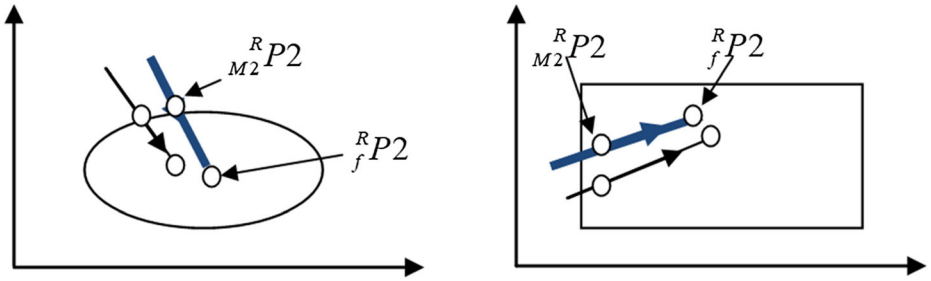

Fig. 11 $^{R}_{M2}P^{M2}2$ and $^{R}_{f}P2$ at the end of inhalation

In light of the above two problems and, according to the depth and location of the puncture location and the respiratory cycle of the patient, the total length of time for the puncture process is firstly set. Generally the puncture time is timed evenly to the whole cycle of physiological movement. The speed of the needle can be calculated by setting the time as mentioned above. In order to synchronize the puncture actuator and the robot arm, the initial point of the puncture actuator should be calibrated, that is, the starting time of the puncture actuator should be set. In this paper, the end time of the respiration is selected as the starting time for the puncture.

The dual channel synchronous control system [13] is designed as shown in the Fig.12. In the synchronous control system, 3rd order polynomial curve fitting and interpolation have been adopted to calculate the motion rule for the puncture needle at all times.

It is known that a PID control algorithm can meet the needs of the control stage during the movement of the puncture mechanism.

In the robot's control system, the moment feedback control method has been adopted to control the robot's system.

The motion of the robot and the motion of the puncture actuator are synchronized, based on the same planning time step derived from the path planning clock, t_robot.

The distance D between the insertion point P_{IN} and the needle tip P_{NT} is unknown and varies and the acquisition of all the parameters is delayed. Therefore it is difficult to know P_{NT} in the coordinate system O_{CT} at any time during the surgical process.

According to the above process, a synchronous controller was added to the control system, and the synchronizer design has been shown in Fig. 13.

Where:

P_{IN}	The location of the insertion of the needle point
P_{NT}	The location of the needle tip
D	The distance between P_{IN} and P_{NT}
$^{R}_{R}P$	The location of the robot in the coordinate system O_R
D'	The location between P_{IN} and P_{NT} computed by the ILC
$^{R}_{R}P'$	The location $^{R}_{R}P$ computed by the ILC
z^{-k}	The delay time
D''	The location obtained by 3rd order polynomial curve fitting and interpolation between P_{IN} and P_{NT}
$^{R}_{R}P''$	The location $^{R}_{R}P'$ obtained by 3rd order polynomial curve fitting and interpolation
C_A	The controller of the puncture actuator

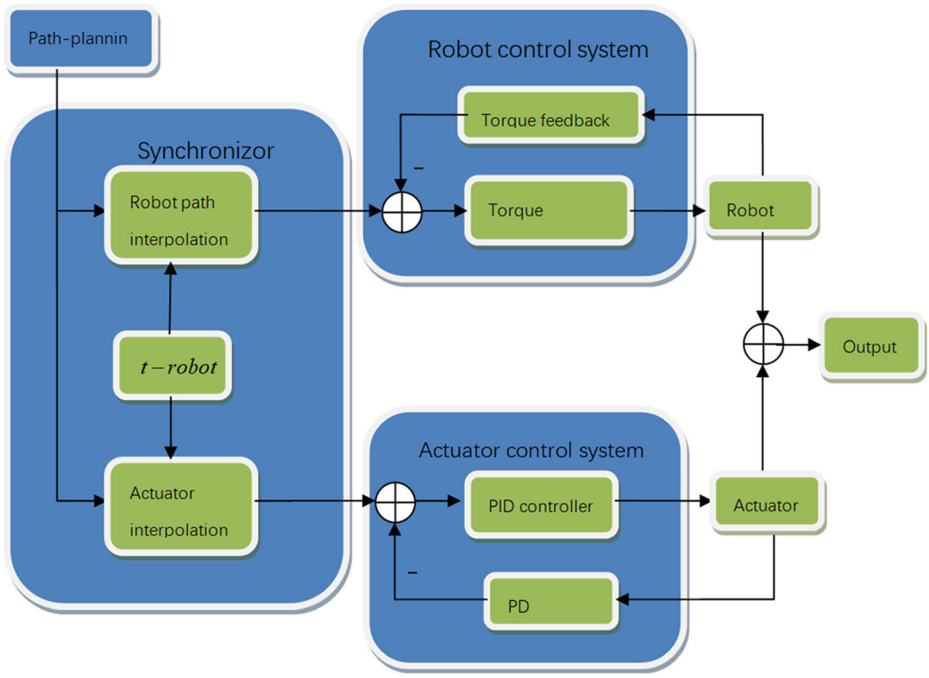

Fig. 12 The control system

Fig. 13 The synchronizer

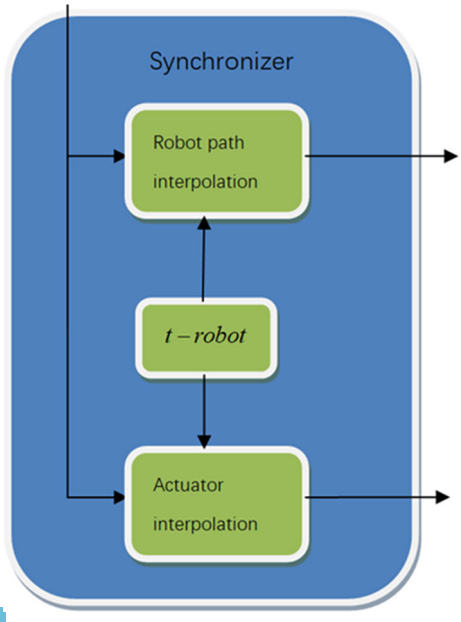

C_R The controller of the robot
A The puncture actuator
R The robot

$^{R}P_{NT} = D''z^{-k}C_A A + {}^{R}_{R}P''\}C_R R$
t The total execution time of the control system
$t = n \times t\_robot, n > 2$, where n is even.

t_robot The total time series of the puncturing
t_robot is an even number of times of the respiratory cycle T and planned during path planning
T' delay time, $T' = {}^{T}/_{2}$

In the synchronizer, a delay module was also set up, at the time that the robot is just starting, the system has not yet become stable, and the robot needs a small period of time to become stable. The time t_robot of the delay module can be set according to the difference of the puncture actuator. During this time, the robot runs increasingly steadily and periodically moves on the designed trajectory.

When the control system starts, the laser sensor measures the amplitude of the physiological motion. The wave peak time is the trigger signal. After the system accepts the signal, the control system starts to work, and the delay module starts to work. When the delay module z^{-k} ends, the puncture actuator moves, and the robot works in collaboration with the puncture actuator. The tip of the needle actuator will move along the planned path.

Within the control system, the needle driving system of the puncture actuator is driven by a simple linear motor. The PD feedback closed-loop control system is suitable for the system above that is mature and has high precision.

The torque feedback control method is used in the control system of the robotic arm, because the position and orientation of the robotic arm are different at every moment, and even the effect of Gravity and the Coriolis force of the robotic arm may be different at any time. Then the output acceleration is calculated by the RNE module (Tables 1 and 2).

8 Simulation

In this paper, MATLAB software was used for modeling and analysis. The location of the robot's joints and the actuator at the final time are shown in the Table 1. The expectation

Table 1 The location of the robot's joints and the actuator at the final time

Actuator	0.02959
Robot joint	0.9358
	0.02861
	−2.522
	−3.708
	1.747
	4.805

Table 2 The expectation location of the robotic joints and the actuator at the final time

Actuator	0.02244
Robot joint	0.9348
	0.03021
	−2.524
	−3.707
	1.749
	4.806

location of the robotic joints and the actuator at the final time are shown in the Table 2.The performance was shown in the Table 3.

Here, points of the path planning system were set as follows: the point of external ${}^{R}_{M2}P^{M2}2$was set as A1 (0.26,0.27,0.185) and ${}^{R}_{M2}P^{M2}1$was set as B1 (0.25,0.26,0.3) at the end of expiration in the global coordinate; the internal point of the body ${}^{R}_{f}P1$was set as A2 (0.3,0.305,0.2) and ${}^{R}_{f}P2$was set as B2 (0.2,0.2,0.1) at the end of inhalation in the global coordinate.

A PD type of the ILC algorithms was used in the control system. *Kp*,*Kd*and Gain were set as (0.05 10 100 5 4000 100), (1.5 10 100 2 40 20) and (0 0 0 0 0 0). The parameters of the actuator were set as Kp_motor=0.1,and Kd_motor=−10. These parameters were set based on characteristics of both the robotic arm and the actuator. The speed and accuracy of path planning can been changed through changing these parameters mentioned above.

Timer parameter t_robot was set as follow: $t\_robot = 4s$. t_robot was the only timer and used by both the control systems above. And the dual channel control systems are triggered at the same time. The each step length of the timer is the same in dual channel control systems.

PID_Kp,PID_Kd,$Kp_robot$and Kd_robot were set as followed: PID_Kp=20, PID_Kd=5, Kp_robot=3000,and Kd_robot=1500.The robotic arm channel performance can be controlled by Torque feedback controller through changing $PID_Kp$and PID_Kd. The actuator channel performance can be controlled by PID-controller through changing Kp_robot and Kd_robot (Fig. 14).

Figure 15 has shown the performance accuracy under different iterations and the positional accuracy of the puncture needle of the actuator at the last iteration. It was seen that the simulation accuracy of the path planning expectation and control process is less than 0.05 mm for the 20th iteration.

Table 3 Errors of the robotic joints and the error of the actuator

Actuator	0.00715
Robot joint	0.000971
	−0.001607
	0.002572
	−0.22117
	0.002008
	−0.0004468

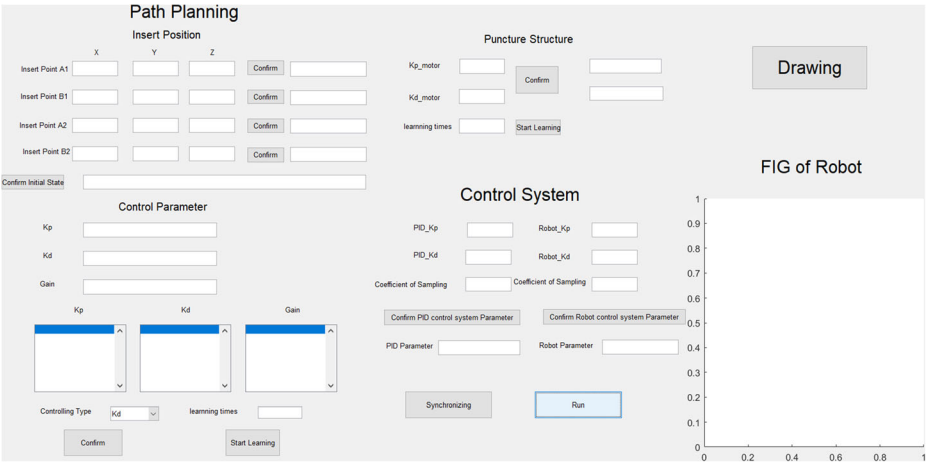

Fig. 14 The interface of the robotic system procedure

Figure 16 has shown the error convergence state of the six joints. After 2 min, the errors were basically unchanged and the system was stable.

Figures 17, 18, 19, 20, 21 and 22 have shown the performance accuracy of each joint at different iterating processes, and the positional accuracy of robotic joints at the last iteration. It was seen from Table 3 that the simulation accuracy of the path planning expectation and control process is less than 0.2 mm after the 20th iteration.

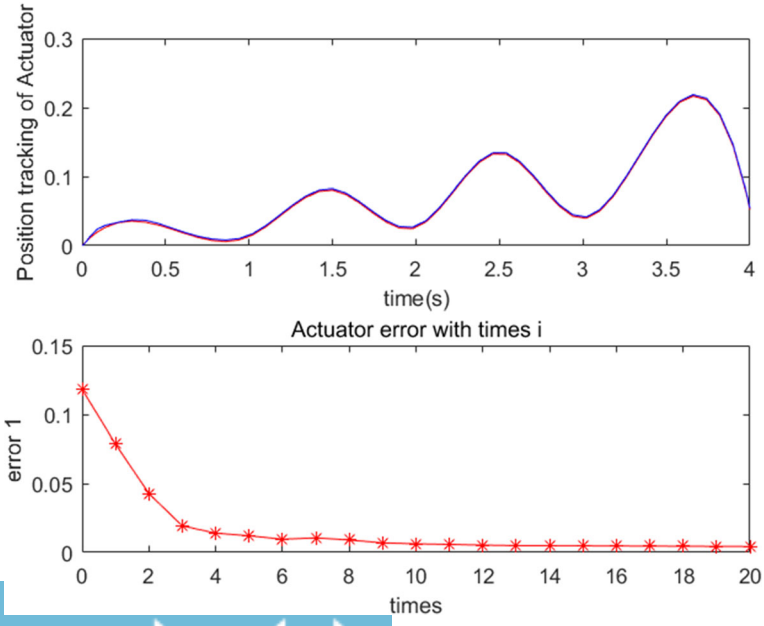

Fig. 15 The tracking process of the trajectories and the error convergence process of the actuator

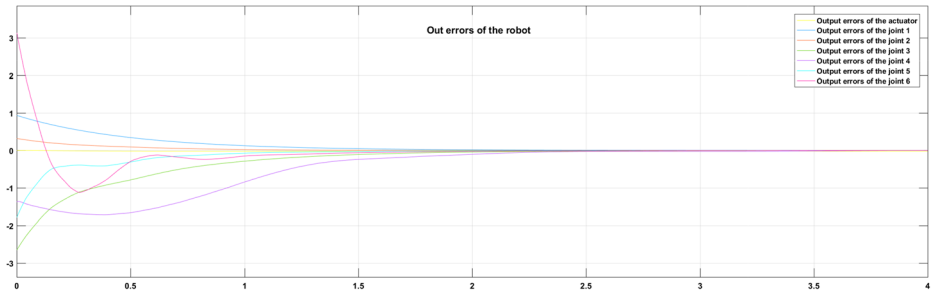

Fig. 16 The error convergence process of the robot's six joints between the control system output and the path planning output

The influence of the accuracy of the first three joints is greater than the accuracy of the last three joints in the spatial position. The first three joints should be considered. As shown in the Table 3, it could be seen the maximum error absolute was 0.22117 at the fifth joint, and that the other joint errors were smaller. The location error of the sixth robotic joint was 0.0004468, compared to the input location of joint 6th.

The advantage of the control system was that two different controller can be synchronize by a synchronous timer based on Iterative Learning Control (ILC) path planning. The control system can compensate the external point (the needle inserting point) movement and synchronize the internal point (focus point) at the same time respectively. The accuracy is higher because of iteration times 20. In the operation, the path planning efficiency can be improved as the Iterative Learning times should be reduced appropriately. That is also, path planning learning would be completed in a short time, and then the operation can be fast carried out by doctors.

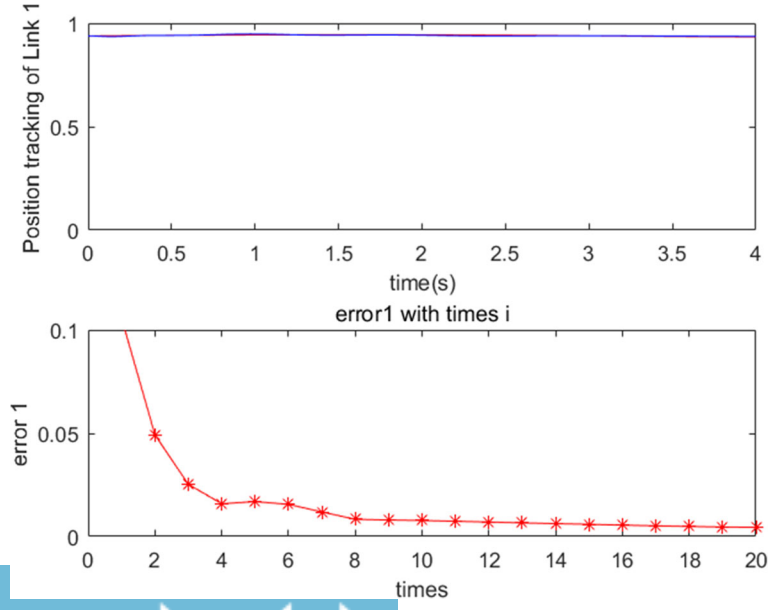

Fig. 17 The first joint position and the error

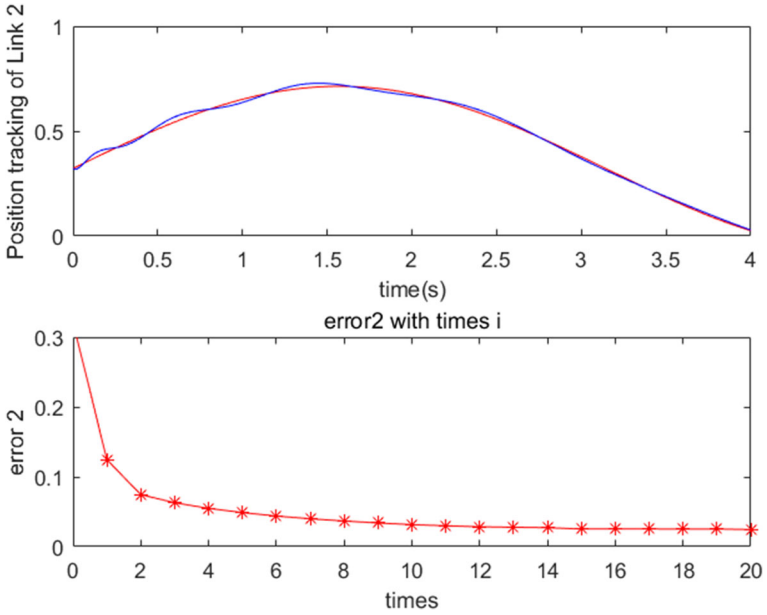

Fig. 18 The second joint position and the error

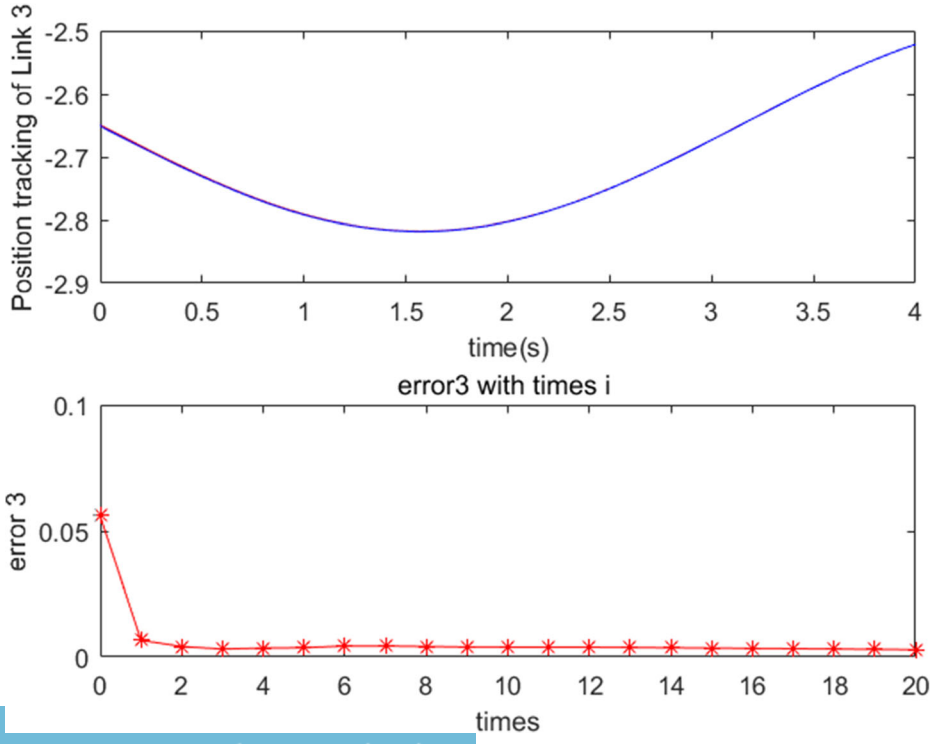

Fig. 19 The third joint position and the error

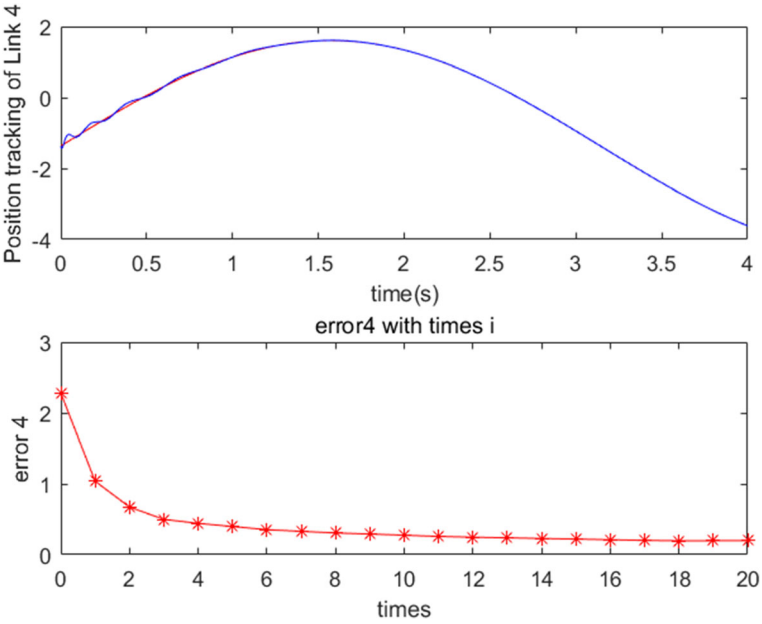

Fig. 20 The forth joint position and the error

In Figs. 15, 16, 17, 18, 19, 20, 21, and 22 the tracking process of the trajectories and the error convergence process of the robot's six joints for the 20th iteration of the path planning have been shown.

In Figs. 17, 18, 19, 20, 21, and 22 the errors of the robot's puncture joints have been shown.

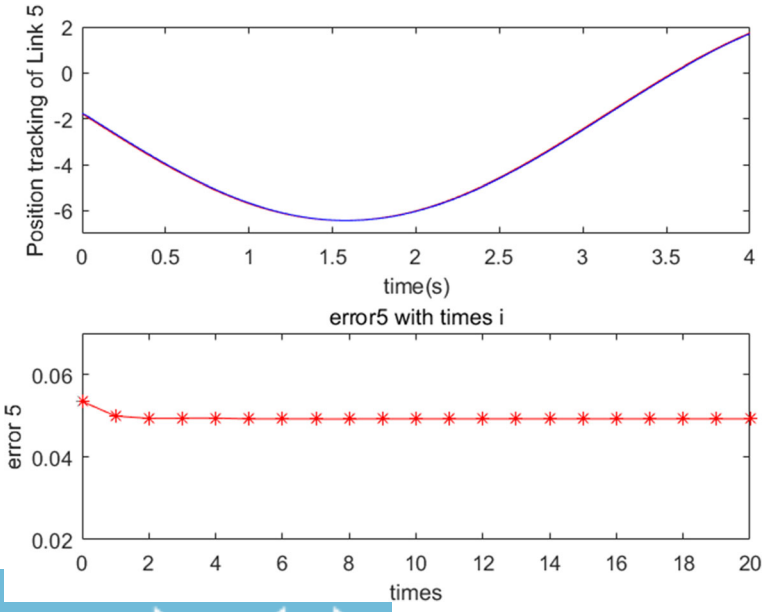

Fig. 21 The fifth joint position and the error

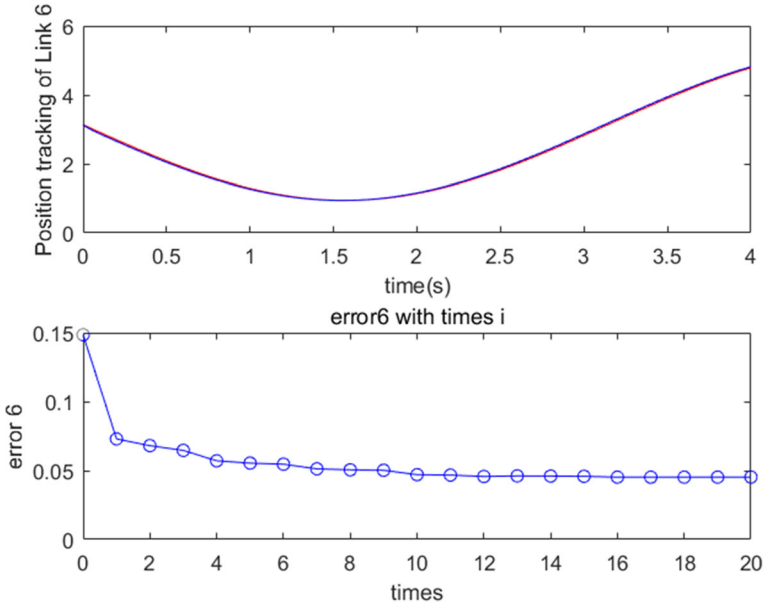

Fig. 22 The sixth joint position and the error

9 Conclusions and future work

In this paper, a dual channel Iterative Learning Control (ILC) algorithm for path-planning and a dual channel control system and a synchronizing controller have been proposed.

Through simulation analysis in the path planning stage, it has been shown that the robot arm and the puncture actuator can successfully learn the needle path through effective path-planning.

In the control system, a synchronization controller was added. The synchronization setting was based on the time step of the robot and the delay time setting was also proposed. The merging of the position and orientation for the above two systems can be finally realized in the synchronization step, so that it can effectively synchronize with the physiological movement of the patient and compensate for the movement caused by breathing and the heart beating. The paths of the robot and the puncture actuator were also fitted and interpolated during the synchronization stage. The precision of the control system outputs is sufficient for the system needs.

In the process of carrying out the puncture, which is automatic and supervised on-line, outside interference is minimal. Online supervision of the automatic insertion system is a new control system for the percutaneous puncture robot. A method and a research direction have been provided in this paper for the automatic surgical procedure system.

References

1. Alexandre B, Zhou J, Yang G et al (2009) Motion compensated tomography reconstruction of coronary arteries in rotational angiography[J]. IEEE Trans Biomed Eng 56(4):1254–1257
2. Bruno D, Calinon S, Caldwell DG (2017) Learning autonomous behaviours for the body of a flexible surgical robot[M]. Kluwer Academic Publishers
3. Cagneau B, Zemiti N, Bellot D, et al. (2007) Physiological motion compensation in robotized surgery using force feedback control[C]// IEEE international conference on robotics and automation. IEEE, 1881–1886

4. Dominici M, Rui C. (2014) Cascade robot force control architecture for autonomous beating heart motion compensation with model predictive control and active observer[C]// biomedical robotics and biomechatronics. IEEE, 745–751
5. Ginhoux R, Gangloff J, Mathelin MD et al (2005) Active filtering of physiological motion in robotized surgery using predictive control[J]. IEEE Trans Robot 21(1):67–79
6. Huang SY (2003) Synchronized moving aperture radiation therapy (SMART): average tumour trajectory for lung patients. Phys Med Biol 48(5):587–598
7. Inoue T, Matsuno T, Yanou A, et al. (2014) Development of a minimally invasive robotic interventional radiology for treatment of lung cancer -manufacture of a basic mechanism and verification experiment-[C]// Sice conference. IEEE, 2646–2651
8. Kobayashi Y, Moreira P, Liu C et al (2011) Haptic feedback control in medical robots through fractional viscoelastic tissue model[J]. Conf Proc IEEE Eng Med Biol Soc 2011(4):6704–6708
9. Ligorio G, Sabatini AMA (2015) Novel Kalman filter for human motion tracking with an inertial-based dynamic inclinometer[J]. IEEE Trans Biomed Eng 62(8):2033–2043
10. Murphy MJ (2004) Tracking moving organs in real time.[J]. Semin Radiat Oncol 14(1):91
11. Nakamura Y, Kishi K, Kawakami H. (2001) Heartbeat synchronization for robotic cardiac surgery[C]// proc. Of IEEE international conference on robotics and automation. 2014–2019 vol.2
12. Prakosa A, Sermesant M, Allain P et al (2014) Cardiac electrophysiological activation pattern estimation from images using a patient-specific database of synthetic image sequences[J]. IEEE Trans Biomed Eng 61(2):235–245
13. Qu J, Li J, Zhang L, et al. (2013) Design of a novel force-reflecting haptic device for minimally invasive surgery robot[C]// ICME international conference on complex medical engineering. IEEE, 357–362
14. Richa R, Bó APL, Poignet P (2010) Beating heart motion prediction for robust visual tracking[C]// IEEE international conference on robotics and automation. IEEE, 4579–4584
15. Sharifi M, Salarieh H, Behzadipour S, Tavakoli M (2017) Tele-echography of moving organs using an Impedance-controlled telerobotic system [J] mechatronics, 05
16. Strååt SJ (2012) Verification of high energy photon therapy based on PET/CT imaging of photonuclear reactions[J]. Department of Physics
17. Vidal FP, Villard PF (2016) Development and validation of real-time simulation of X-ray imaging with respiratory motion[J]. Computerized Medical Imaging & Graphics the Official Journal of the Computerized Medical Imaging Society 49:1–15
18. Wood NA, Agua DMD, Zenati MA, et al. (2011) Position estimation of an epicardial crawling robot on the beating heart by modeling of physiological motion[C]// Ieee/rsj international conference on intelligent robots and systems. IEEE, 4522–4527.
19. Zarrouk Z, Chemori A, Poignet P (2013) Force feedback control for compensation of physiological motions in beating heart surgery with real-time experiments[J]:956–961

Liandong Wang , is pursuing his Ph.D degree in Department of Mechanical Manufacture and Automation. School of Mechanical and Aerospace Engineering (SAME). Jilin University (JLU). His research interests include medical robot, control system, robotics structure.

Tiehua Hu , is working in China Academy of Machinery Science & Technology (CAM). She is now a professor in the CAM. Her research interests include signal processing, control system, non-destructive testing technology.